Automatic Location of Sources of Electrical Activation from Electroanatomical Maps

Fernando Barber, Miguel Lozano, Ignacio García-Fernández, Rafael Sebastian

CoMMLab, Universitat de Valencia, Valencia, Spain

Abstract

Electro-anatomical mapping is a widely used technique used by electrophysiologists to understand patient's activation pattern. The system measures activation time at different locations but does not provide information on underlying electrical pathways or triggering points, such as Purkinje-myocardial junctions or ectopic foci. We present a method to estimate the locations of Purkinje-myocardial junctions from a discrete set of endocardial samples. Using less than 1000 endocardial samples it can recover locations and activation times of the most influencing Purkinje myocardial junctions from Purkinje trees of up to 500 junctions. A simulation study revealed that using the estimated Purkinje myocardial junctions, mean squared errors of local activation times remain low for different tree structures.

1. Introduction

The heart electrical sequence of activation in healthy subjects is deterministic and can be monitored by means of the ECG. In the ventricles, the activation of the myocardial muscle is triggered by Purkinje-myocardial junctions (PMJs), which are the terminal sites of the specialised cardiac conduction system (CCS) [1]. However, the location and density of PMJs is expected to vary between subjects, given the stochastic nature of the CCS development at distal regions [2]. Several important cardiac disorders such as ventricular dyssynchrony or ventricular tachycardia (VT) [3], require therapies that could interact directly with the CCS, such as cardiac resynchronization therapy (CRT) [4], radiofrequency ablation or antiarrhythmic drugs [5].

Developing patient-specific CCS models is key for cardiac electrophysiology and electromechanical simulation in health and disease [6]. To simulate the activation sequence of a patient a model with tailored CCS structure and PMJ distribution is required. In addition, knowing the location of dense PMJs areas can help in the delivery of electrical therapies, e.g. by better selecting the location of CRT leads to minimize the time to reach the CCS, or by avoiding ablating by RFA regions with a high density of PMJs.

Despite the well-known importance of the CCS [7], the challenges associated to obtaining its structure in vivo have led modellers to use simplified approaches to reproduce its function. Among the most common methods to build generic CCS for cardiac modelling there are: manual delineation of CCS branches, fractal models, segmentation of free-running sections from high-resolution ex-vivo images, or stochastic rule-based CCS models constrained by population ex-vivo animal data [8]. Since it is not possible to obtain direct in-vivo imaging data from the CCS structure, the only related data available are the electrical measurements obtained by electro-anatomical mapping systems (EAMs). Recently, two different studies have tried to use EAM data to generate CCS's able to better reproduce the patient's sequence of activation compared to a generic CCS [9, 10]. However, none of them tries to estimate the real location of PMJs, but only a compatible activation sequence.

This study presents a method to estimate the location and activation time of all relevant endocardial sources of electrical activity (PMJs and/or ectopic foci) from a discrete set of endocardial samples obtained from an EAM. The method is based on knowledge about the way that the electrical wavefront propagates on tissue. To be able to validate the method we use a simplified domain were the complexity of the CCS, the number of PMJs and number of samples can be controlled. Given a minimum ratio of EAM samples versus PMJs the system will locate trigger points with an error in the order millimetres.

2. Material and methods

2.1. Estimation method

We aim to estimate the location, s, and activation time τ of a set of PMJs, $\mathcal{P}$, from a set of sample points, $\mathcal{M}$, which are tuples $(x_i, t_i) \in \Omega \times \mathbb{R}$, where $\Omega \subset \mathbb{R}^2$ represents space in the endocardial domain, and $i=1,\ldots,m$ (see Figure 1). In Ω the activation time, t, of a point x can

be calculated as,

$$t(x) = \min_k(\tau_k \frac{||x-s_k||}{v}), \quad (1)$$

where v is the propagation velocity in the myocardium and k =*1,…,n*. The location and number of PMJs, n, in the set $\mathcal{P}$ is unknown and has to be estimated.

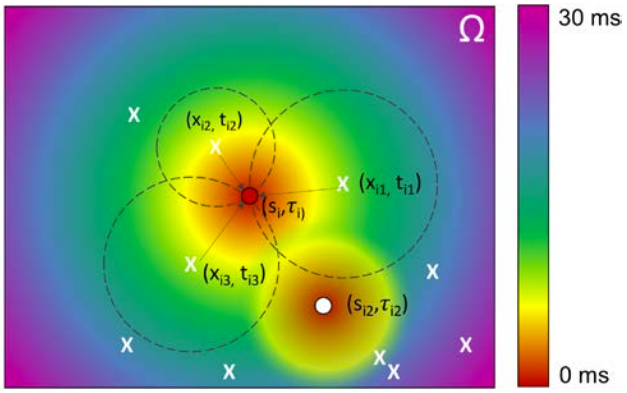

Figure 1: Color-coded endocardial domain activated by two PMJs, depicted as small circles, at t=0 ms. White crosses are sample points from the set $\mathcal{M}$, similar to those obtained in EAMs.

The activation generated by each PMJ can be considered as a positive half cone with its vertex at (s, τ), so that all points (x, t) within that cone are activated by the same PMJ, meeting the following equation,

$$||x - s|| = v(t - \tau). \quad (2)$$

If three different points from $\mathcal{M}$ are activated by the same PMJ, each of them must meet Equation 2 for the same cone vertex.

To estimate the PMJs locations, we arrange all points in $\mathcal{M}$ in groups of three points. First, we perform a Delaunay triangulation assuming that points close in space might have a higher probability of being activated by the same PMJ. As a second step we solve the system of non-linear equations defined for the three points of each triangle using Equation 2. Since each PMJ propagation defines a half cone, it must also meet that $t_i > \tau$ for *i=1,..,3*. In addition, it is required that the estimated PMJ is compatible with the backward Eikonal problem associated to the triangle where the estimated PMJ is located in.

2.2. Simulation study

To test the methodology, we developed a simulation study based on synthetic Purkinje trees with different branch and PMJ densities. All the Purkinje trees lie on a 2D sheet of tissue of 7x12cm that represents the endocardium. To build the Purkinje tree structure we use an algorithm that creates branches recursively up to a user defined level depth. As depicted in Figure 2, at each level branches grow from terminal points and are perpendicular to previous level branches. Terminal nodes at the deepest level of recursion are considered the PMJs. Branch lengths are generated following a normal distribution with parameters obtained from [8].

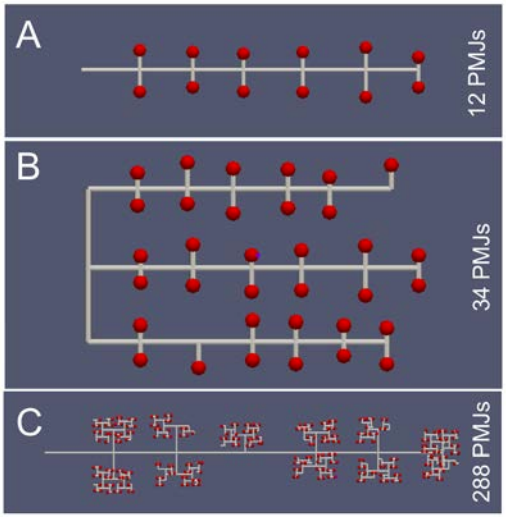

Figure 2: Three different configurations of the CCS with increasing density of PMJs (red spheres). Configurations used can have one primary branch (A) and (C), or three primary branches (B).

In this study we used three different levels of branch recursion, 2, 4 and 6.

For each scenario we generated 10 different sets of random sample points $\mathcal{M}$ on the 2D tissue sheet. The size of the sets varied from 100 to 1000 points in steps of 100, and were used to estimate PMJ locations and activation times. The size of the set $\mathcal{M}$ is in the order of magnitude of a routinely EAM acquired in the clinic. The activation time at sample points was determined using a forward simulation and can be calculated by Equation 1. Figure 3 shows an example of a Purkinje configuration, where red spheres represent the PMJs, and crosses the sample points.

We defined the parameters for six different Purkinje tree configurations, and produced 10 instances for each of them. Following, we estimate the PMJ locations using an increasing number of sample points. Finally, from the estimated PMJs, we propagate the electrical wavefront to the tissue and calculate the mean square error of the local activation times.

3. Results

The results of the PMJ estimation are graphically represented in Figure 3. It corresponds to a simulation with 3 main branches, and a recursion depth of 2, which produced 34 PMJs. In that simulation, 4 PMJs were not

detected, 30 were properly estimated, and 1 was incorrectly estimated (red arrow). The regions encircling sample points indicate that all samples within are pointing to a single PMJ candidate. In some special configurations where there are many sample points, the algorithm can resolve a plausible alternative location for a PMJ given the input data, which does not correspond to the real one. For that reason, we perform additional checks to the solver solution, to report also the PMJs correctly estimated.

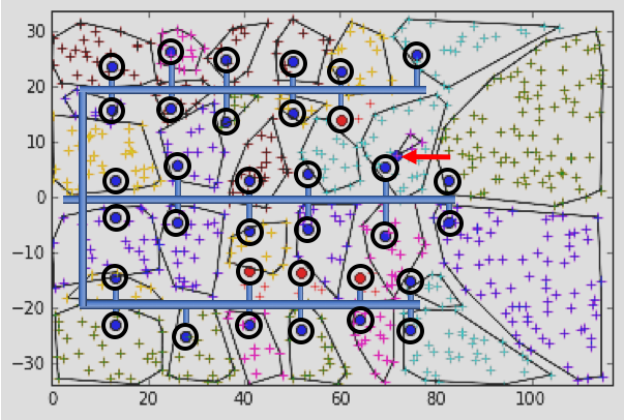

Figure 3: Configuration with three main branches and 34 PMJs (black circles), together with a random set of sample points (crosses). Blue dots mark the location of automatically properly estimated PMJs. Red dots within PMJs correspond to undetected PMJs. Red arrow points to an incorrectly estimated PMJ.

Figure 4 shows results for two representative Purkinje tree configurations. Each plot shows the mean number of PMJs for the scenario (10 repetitions per scenario), the number of effective PMJs (which can be truly estimated from the samples), the total number of PMJs estimated by the algorithm and finally, the number of PMJs correctly estimated.

In scenarios with 15-45 PMJs (0.28-0.83 PMJs/cm^2) and a reasonable level of clustering, the algorithm obtains nearly all PMJs (see Figure 4a) when it has enough sample points, that is more than 700. However, when the density of PMJs increases to around 100-200, the problem becomes more complex, since these points tend to be clustered. If we take into account only the effective PMJs, that is those that activate some tissue (detectable), then the number of PMJs decrease to around 80-90. From those, the algorithm is able to detect 50-60 PMJs when 1000 sample points are used (see Figure 4b).

Despite the limitations in the detection algorithm, when the estimated PMJs are used to activate the tissue, the LAT errors obtained are small as shown in Figure 5. Having 300 sample points or more the MSE calculated on the LATs is low in most of the scenarios. The densest cases with around 500 PMJs requires at least 600 sample points to ensure that LATs produced by the estimated PMJs are close to real ones.

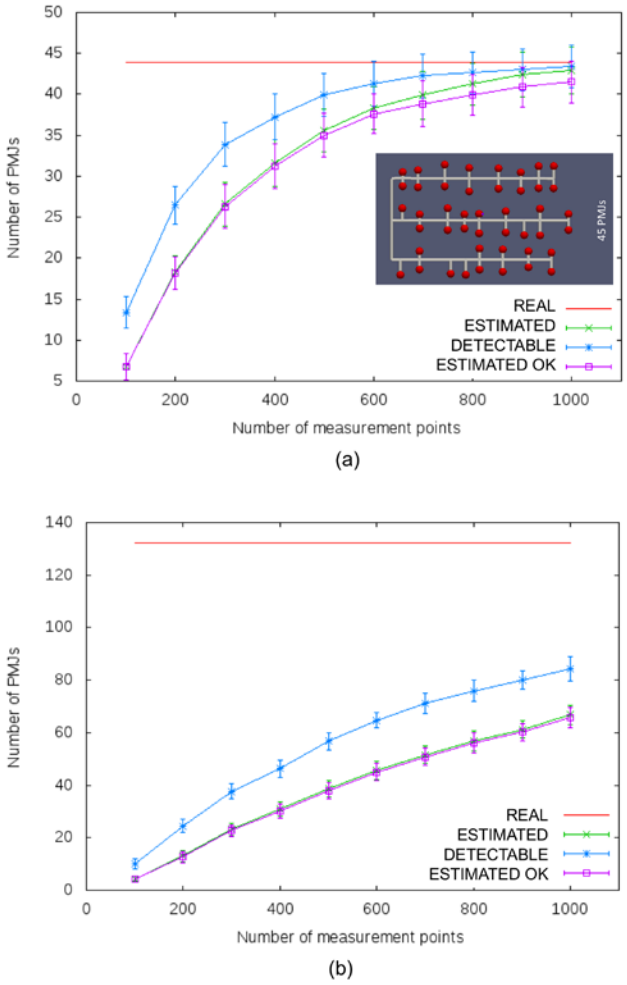

Figure 4: Detected PMJs for two configurations with three primary main branches and an increasing number of sample points; (a) using a recursion depth of 2 (average 35.4 PMJs), and (b) a recursion depth of 4 (average 132.2 PMJs). REAL are the real PMJs in the tree, ESTIMATED are those detected by the solver, DETECTABLE are those activating a minimum amount of tissue that can be detected from the sample points and ESTIMATED OK, which are those correctly estimated after applying all the check.

4. Discussion and conclusions

We have presented a method to estimate the location and activation time of PMJs from a set of random sample points, to emulate the data acquired in a clinical electro-anatomical map.

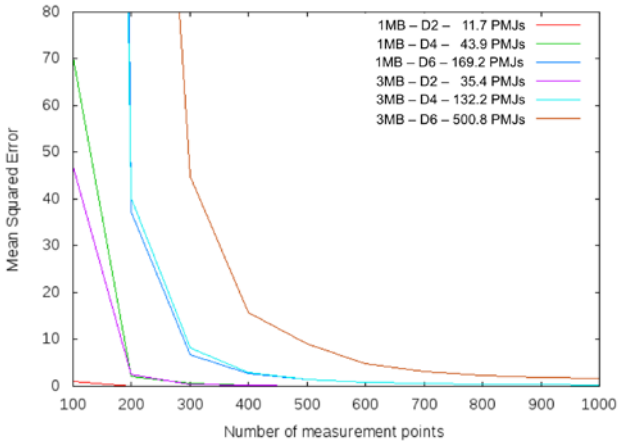

Figure 5: Mean squared LAT error (in ms) obtained for different scenarios (10 repetitions), where the estimated PMJs are used to activate the tissue. PB stands for the number of primary branches, as depicted in Figure 2, and D for recursion branch depth.

We show that given an appropriate ratio between the number of PMJs and endocardial samples acquired, the system can locate the effective PMJs and determine their activation time, provided that they are not arranged in small clusters. In order to detect all PMJs, we will need to sample, at least, with a density three times higher than the highest density of PMJs. When clustered PMJs appear, they are virtually impossible to be detected with the current setup. The signal emitted by inner PMJs is quickly masked by the PMJs in the cluster border and therefore their effect on tissue is very limited or even non-effective at all. PMJ located in cluster borders are properly detected, while the inner PMJs are in general missed by the algorithm. This fact is very clear when analyzing the MSE of the LATs in the sample points. From these results, we conclude that our algorithm is capable of finding most of the effective nodes of the cardiac conduction system.

The method presents some limitations that have to be addressed. Of particular relevance is that it neglects the existence of any electrical barrier in the endocardial tissue which can be produced by ischemia or a lesion generated during a RFA procedure. The current study has been carried out considering that endocardium is isotropy or presents a fix anisotropy, which does not change throughout the domain.

Acknowledgements

This study is supported by the e3DTorso project (TIN2014-59932-JIN) from the Spanish Ministerio de Ciencia y Competitividad and FEDER funds.

References

[1] S. Tawara, Das reizleitungssystem des säugetierherzens. Eine anatomisch-histologische studie über das atrioventricularbündel und die purkinjeschen fäden. Jena, Germany: Verlag, 1906.

[2] Dobrzynski H, Anderson RH, Atkinson A, Borbas Z, D'Souza A, Fraser JF, Inada S, Logantha SJRJ, Monfredi O, Morris GM, Moorman AFM, Nikolaidou T, Schneider H, Szuts V, Temple IP, Yanni J, Boyett MR. Structure, function and clinical relevance of the cardiac conduction system, including the atrio ventricular ring and outflow tract tissues. Pharmacol. Ther. 2013; 139(2), 260–288.

[3] Haissaguerre M, Vigmond E, Stuyvers B, Hocini M, Bernus O. Ventricular arrhythmias and the His-Purkinje system, Nat Rev Cardiol, 2016; 13(3):155-166.

[4] Kimmel MW, Skadsberg ND, Byrd CL, Wright DJ, Laske TG, Iaizzo PA. Single-site ventricular and biventricular pacing: investigation of latest depolarization strategy. Europace. 2007; 9(12):1163-70.

[5] Dux-Santoy L, Sebastian R, Felix-Rodriguez J, Ferrero JM, Saiz J. Interaction of specialized cardiac conduction system with antiarrhythmic drugs: a simulation study. IEEE Transactions on Biomedical Engineering, 2011; 58(12):3475-78.

[6] Vigmond EJ, Stuyvers BD. Modeling our understanding of the His-Purkinje system, Progress in Biophysics and Molecular Biology, 2016; 120(1–3):179-188.

[7] Atkinson A, Inada S, Li J, Tellez JO, Yanni J, Sleiman R, Allah EA, Anderson RH, Zhang H, Boyett MR, Dobrzynski H. Anatomical and molecular mapping of the left and right ventricular His Purkinje conduction networks. J. Mol. Cell. Cardiol, 2011; 51(5):689-701.

[8] Sebastian R, Zimmerman V, Romero D, Sanchez-Quintana D, Frangi AF Characterization and Modeling of the Peripheral Cardiac Conduction System. IEEE Transactions on Medical Imaging, 2013; 32(1):45 – 55.

[9] Cardenes R, Sebastian R, Soto-Iglesias D, Berruezo A, Camara O. Estimation of Purkinje Trees from Electro-Anatomical Mapping of the Left Ventricle Using Minimal Cost Geodesics. Medical Image Analysis, 2015; 4(1):52 – 62.

[10] Vergara C, Palamara S, Catanzariti D, Nobile F, Faggiano E, Pangrazzi C, Centonze M, Maines M, Quarteroni A, Vergara G. Patient-specific generation of the Purkinje network driven by clinical measurements of a normal propagation. Med Biol Eng Comput, 2014; 52(10):813-26

Address for correspondence:
Rafael Sebastian
Office 1.2.22. Computational Multiscale Simulation Lab (COMMLAB), Universitat de Valencia. Escuela Técnica Superior de Ingenierías. Av. de la Universidad s/n, 46100 - Valencia (Spain).
rafael.sebastian@uv.es